

A New Polystyrene-based Ionomer/MWCNT Nanocomposite for Wearable Skin Temperature Sensors

Alessio Giuliani,¹ Massimo Placidi,² Fabio Di Francesco,^{1,3} Andrea Pucci,^{1,3}

¹Dipartimento di Chimica e Chimica Industriale, Università di Pisa, Via Risorgimento 35, 56126 Pisa, Italy;

²HORIBA Jobin Yvon S.r.l., Via Cesare Pavese 19/21 - 20090 Opera, Milano, Italy

³INSTM, Unità di Ricerca di Pisa, Via Risorgimento 35, 56126 Pisa, Italy

Corresponding author:

Dr. Andrea Pucci

Dipartimento di Chimica e Chimica Industriale, Università di Pisa, Via Risorgimento 35, 56126 Pisa, Italy. Tel: +39 050 2219270; Fax: +39 050 2219 260; Email: apucci@dcc.i.unipi.it

Abstract

The present work outlines the fabrication and testing of a novel skin temperature sensor based on exfoliated and undamaged multi-walled carbon nanotubes (MWCNTs) dispersed in a poly(vinylbenzyl chloride) derivative with triethylamine (PVBC_Et₃N). The dispersions were prepared by sonicating MWCNT/PVBC_Et₃N mixtures in dimethylformamide for 5 min and the quantification of the MWCNTs dispersed was evaluated by UV-vis spectroscopy investigations and thermogravimetric analyses.

The investigations demonstrated the realization of MWCNT/PVBC_Et₃N sensors with a resistance sensitivity to temperature close to -0.004 K^{-1} , an absolute value that is comparable to the highest values found in metals. The temperature dependence of the resistance was also found very reproducible in the range 20-40 °C, thus suggesting the possibility of using the MWCNT/PVBC_Et₃N system as for the fabrication of small wearable temperature sensors to be used for the monitoring of chronic wounds.

Keywords: MWCNTs, poly(vinylbenzyl chloride) ionomers, MWCNT dispersion, electrically conducting nanocomposite, wearable temperature sensor

1. Introduction

Carbon nanotubes (CNTs) are a third allotropic form of carbon brought to the forefront by the pioneering work of Iijima et al. in 1991.[1] CNTs represent a dominant class of nanostructured materials whose unique mechanical, electrical and thermal properties depend critically on their structural perfection and high aspect ratio (typically $>10^2$).[2-4] Single-walled CNTs (SWCNTs) consist of single graphene sheets (monolayer of sp^2 bonded carbon atoms) wrapped into cylindrical tubes with a diameter ranging from 0.7 to 2 nm and lengths up to micrometers. Multi-walled CNTs (MWCNTs) consist of concentric assemblies of SWCNTs and are therefore characterized by larger average diameters. The exceptional properties shown by SWCNTs and MWCNTs support the virtues of their incorporation into polymeric matrices to produce nanocomposites for a variety of applications, ranging from strong and lightweight materials to nanometer-sized electronic devices and electrochemical sensors.[2, 5-9]

However, even if CNTs potentially represent one of the most important filler materials for polymers, their utilization is problematic due to the strong van der Waals interactions between individual nanotubes, which hinder a uniform dispersion at the nanoscale level. Ultrasonication of CNTs mixtures containing the desired polymer is mostly used for unbundling CNTs, even if significant damage of their structures as well as shortening occur, which limit the full potential of CNTs as additives in polymers.[10]

We have recently investigated the influence of the sonication time on the characteristics of MWCNTs dispersions within poly(styrene-*b*-(ethylene-co-butylene)-*b*-styrene) (SEBS) mixtures for the realization of miniaturized temperature sensors.[11, 12] We demonstrated that a sonication time higher than 30 min induced an extensive MWCNTs degradation (average length decreased of about 40%), which affected the electrical conductivity of the nanocomposites. On the other hand, the use of alkyl-functionalized MWCNTs appeared to be more effective in preparing SEBS nanocomposites due to the higher dispersion efficiency, negligible nanotube degradation and higher electrical conductivity. The resulting films showed a temperature dependent resistivity with a

sensitivity comparable to the highest values found in metals, which was however partly lost after the first heating cycle up to 55-60 °C.[11] This loss of sensitivity was attributed to the elastomeric nature of the SEBS matrix, whose mobility with temperature did not ensure a phase stability to the dispersed MWCNTs.

In this work, aiming at preparing highly dispersed MWCNT/polymer nanocomposites with a more stable temperature sensitivity in multiple cycles, we selected a polystyrene-based ionomer (a poly(vinylbenzyl chloride) (PVBC) aminated with triethylamine, PVBC_Et₃N) as the continuous polymer matrix. Indeed, the use of surfactants and ionic polymers (ionomers) is well reported in literature for the realization of high concentration, high-quality CNT dispersions for technological applications.[13-15] The ionomers are reported to effectively interact with CNTs through weak van der Waals and cation- π interactions. Once the CNTs are detached during sonication, they are immediately surrounded by the ionic macromolecules thus shielding the strong π - π interactions between CNTs and eventually preventing their rebundling.[16, 17]

PVBC is an ideal, high glass transition temperature (T_g) polymer (~100 °C) to which a variety of functional moieties can be attached by nucleophilic substitutions in mild reaction conditions.[18-21] Moreover, the high T_g of these materials should guarantee the phase stability of CNT nanocomposites in the low temperature regime (20-40 °C), as the application target of the present research is the realization of wearable temperature sensors for the monitoring of chronic wounds.

The dispersions were prepared by sonicating MWCNT/PVBC_Et₃N mixtures in DMF for 5 min, and the amount of dispersed CNTs was quantified by UV-vis absorbance measurements and gravimetric analyses. Atomic force microscopy and Raman spectroscopy were employed to assess the structural integrity of MWCNTs. The temperature dependence of resistance of MWCNT/PVBC_Et₃N nanocomposites was investigated in the range 20-60 °C to explore their potential for the development of linear, stable and reproducible temperature sensors.

2. Materials and methods.

2.1 Materials

All the solvents were either used as received or purified by standard procedures.

4-Vinylbenzyl chloride (VBC) (4-(chloromethyl)styrene, Aldrich, 90%) was purified by washing it twice with a 25 % (v/v) aqueous sodium hydroxide solution, and then thoroughly washed with distilled water until neutral. Finally, the monomer was distilled at reduced pressure and stored under nitrogen over molecular sieves at -20 °C. α,α' -Azobisisobutyronitrile (AIBN) (Carlo Erba) was purified by recrystallization from acetone. Triethylamine (TMA) (Sigma-Aldrich, $\geq 99\%$) was used as received.

Multi-walled carbon nanotubes (MWCNTs, Baytubes C150 P), a generous gift from Bayer Material Science, were used as received. These nanotubes are vapor grown and typically consist of 3-15 graphitic layers wrapped around a hollow 4 nm core. Typical diameters range from 13 to 16 nm, and the lengths are between 1 and 10 μm . The density is approximately 1.4-1.6 g/cm^3 .

2.2 Preparation of PVBC

Poly(vinylbenzyl chloride) (PVBC) was prepared by radical bulk polymerization of VBC in the presence of 1% by mol of AIBN. The solution was stirred at 70 °C for two hours under nitrogen atmosphere, the crude product was then purified by a double dissolution in chloroform and precipitation in methanol and recovered after drying at reduced pressure. The monomer conversion ($\sim 30\%$) was determined off-line via gravimetric analysis and the molecular weight of the sample was evaluated by size exclusion chromatography.

2.3 Preparation of PVBC_ Et_3N

The purified PVBC (0.543 g, 3.56 mmol of VBC repeating units) was dissolved in 20 mL of chloroform in the presence of a two-fold molar excess of Et_3N (1 mL, 0.720 g, 0.712 mmol) and the solution stirred at 60 °C for 24 hours during which the solution became turbid. The reaction mixture was concentrated by evaporating chloroform, and 0.910 g of PVBC_ Et_3N were finally obtained by precipitating the suspension twice in diethyl ether and drying the precipitate under vacuum.

2.4 Preparation and characterization of the MWNT/PVBC_Et₃N dispersions

A stock solution was prepared by dissolving PVBC_Et₃N (0.4 g) in 100 mL of dimethylformamide (100 mL). Aliquots of this solution (5 mL) were poured in vials containing different amounts of MWCNTs, up to a 1:1 weight ratio with PVBC_Et₃N. Uniform dispersions were then obtained by ultrasonication (UP 400 S, Hielscher) the mixtures for 5 min at full power (400 W) and at a frequency of 24 kHz. The immersion of the vials in a water/ice bath allowed us to keep the evaporation of toluene during sonication at negligible levels. The resulting dispersions were centrifuged at 4000 rpm for 30 min and then filtered to remove the residual MWCNT agglomerates. The final MWCNTs/ PVBC_Et₃N weight ratio in the mixture was evaluated by thermogravimetric analysis (TGA) on the dried materials. The MWCNTs wt.% was determined by calculating the ratio between the degradation steps of PVBC_Et₃N (from room temperature to 600 °C) and MWCNT (from 600 °C to 900 °C).

The electric resistance measurements were performed on films obtained by casting 10 µL of the MWCNT/PVBC_Et₃N dispersions in DMF onto a gold electrode pair supported on a 50 µm thick polyimide film (Cad Line, Pisa, Italy). Polyimide was chosen due to flexibility and chemical inertness, which are important constraints for wearable temperature sensors to be used for the monitoring of chronic wounds. Gold electrodes were prepared from copper tracks obtained by photolithography, which were subsequently electroplated with nickel and gold (electrode dimensions: length 7 mm, width 1 mm, distance 2 mm; thickness of copper 35 µm, nickel 3.0 µm, gold 1.2 µm).

2.4 Apparatuses

Infrared spectra were recorded by a Fourier transform infrared spectrometer (Spectrum One, PerkinElmer) on films cast from CHCl₃ or DMF solutions on a KBr window.

Proton magnetic resonance (¹H NMR) spectra were recorded by using a Varian Gemini 300 MHz on 5-10% CDCl₃ (Aldrich, 99.8 atom % D) solutions. NMR spectra were registered at 20 °C and the chemical shifts were assigned in ppm using the solvent signal as a reference. Data analysis was

performed by in-house routines developed on the Igor Pro platform Wavemetrics. Curve fitting was done by least-squares methods using built-in functions in Igor Pro ($R^2 = 0.998$).

The PVBC molecular weight was obtained with high performance liquid chromatography analyses of chloroform-diluted solutions performed by an isocratic pump unit (PU-1580, Jasco), a refractive index detector (830-RI, Jasco) and two organic GPC/SEC columns (PLgel 5 μm MIXED- C, Polymer Laboratories). The calibration curve was obtained with polystyrene standard samples.

The morphologies of MWNTs/PVBC_Et₃N films were examined by a multimode atomic force microscope (AFM, Veeco Metrology, Inc.) equipped with E and J piezoelectric scanners. The instrument was connected to controller and to a signal direct access module (Veeco Metrology Inc. Nanoscope IV) connected to an oscilloscope (TDS 2004B Tektronix).

The ultraviolet–visible (UV-vis) absorption spectra of dispersions were recorded with a UV/vis spectrometer (Perkin-Elmer Lambda 650).

Thermogravimetric scans were carried out by a Mettler Toledo Starc System (TGA/SDTA851°). Samples were heated from 25 to 600 °C at 10 °C/min under a nitrogen flow, and from 600 to 900 °C under an air flow.

Raman spectroscopy was performed using a confocal Raman microscope (Horiba Jobin Yvon Xplora ONE). The wavelength of the excitation laser was 785 nm and the power of the laser was kept below 1mW to avoid any noticeable sample heating. The laser spot size was 1 μm with a 100X objective lens (numerical aperture D 0:90). The signal was acquired using a thermoelectrical CCD cooled down to -50 °C.

Calorimetric analyses were performed under nitrogen flux (80 mL/min) by a differential scanning calorimeter (Mettler-Toledo 822e) equipped with a cooling system. The calibration was performed with Zinc and Indium. Heating and cooling thermograms were recorded at a standard rate of 10°C/min.

The sensitivity to temperature of nanocomposites was evaluated by sandwiching the films between two aluminium plates heated by two mica plate heaters (RS 615-1700, RS Components). A

temperature controller (dTRON 316, Jumo) connected a thermocouple embedded in one of the plates allowed a fine regulation of the set-point temperature. Film resistance was measured by a precision digital multimeter (2700, Keithley).

3. Results and discussion

3.1 Preparation and characterization of PVBC_Et₃N

Poly(vinylbenzyl chloride) (PVBC) was prepared by radical bulk polymerization of VBC in the presence of 1% by mol of AIBN under nitrogen atmosphere. The polymer was characterized by a number- and weight-average molecular weight of 12,000 g mol⁻¹ and 20,400 g mol⁻¹ respectively, and a monomer conversion of about 30 %. The glass transition temperature was about 100 °C.

PVBC was then converted in the aminated PVBC_Et₃N form with a two-fold molar excess of triethylamine. The FT-IR spectra in Figure 1 reveal a significant decrease of the -CH₂Cl and C-Cl stretching bands at 1265 cm⁻¹ and 675 cm⁻¹ and the emergence of the C-N peak at 1370 cm⁻¹ after the reaction of PVBC with Et₃N.

<Figure 1 near here>

The intense band near 1600 cm⁻¹ was attributed to the bending related to absorbed water and indicates the hydrophilic character of the PVBC_Et₃N system.

The ¹H NMR spectrum of PVBC (Figure 2a) displays peaks in the range 7.1-6.5 ppm and 2-0.9 ppm that were referred to the aromatic and aliphatic protons of the VBC repeating units, and a peak at about 4.5 ppm that was attributed to the two chloromethylenic protons of VBC. After reaction with Et₃N, a new broad resonance emerged at 4.4 ppm due to the ammonium nitrogen-linked methylene protons -CH₂-N⁺Et₃ (Figure 2b). This broad and asymmetric peak was caused by a residual contribution at 4.5 ppm due to the unreacted VBC units. Based on peak integrals calculated after a deconvolution analysis (dotted lines, Figure 2b), about 78 % Cl atoms of the benzyl groups in PVBC were replaced by Et₃N.

<Figure 2 near here>

After reaction with Et₃N, the polymer exhibited a T_g of about 125 °C.

3.2 Preparation and characterization of MWCNT/PVBC_Et₃N mixtures

MWCNT/PVBC_Et₃N dispersions were obtained by ultrasonication of precursors in DMF, followed by centrifugation. The ultrasonic device was fixed so that its sonotrode could be reproducibly dipped into the dispersion, which was contained every time in vials of the same volume and shape. An effective refrigeration with a stirred water/ice bath limited the increase in temperature and the loss of solvent to negligible levels.

All CNTs are active in the UV-vis region and exhibit characteristic bands corresponding to 1D van Hove singularities.[22, 23] Therefore, it is possible to establish a relationship between the amount of CNTs individually dispersed in the PVBC_Et₃N DMF mixture and the intensity of the corresponding absorption spectrum. Figure 3 shows the UV-vis absorbance measurements of MWCNT/PVBC_Et₃N DMF dispersions plotted at different MWCNT concentrations obtained after 5 min of sonication. The time of sonication was limited to 5 min to prevent CNTs degradation.[12] In literature, the absorbance spectrum of CNTs reveals intense absorption peaks at 255 and 273 nm attributed to bulk π -plasmon and surface excitations, respectively.[24] As a result of the strong overlapping spectral features of PVBC_Et₃N and DMF, the cut-off was necessarily positioned at 320 nm. The absorbance spectrum of pure PVBC_Et₃N in DMF solution does not display any significant absorption over the entire wavelength region of 320-500 nm.

During sonication, the dissipated mechanical energy overcomes the van der Waals interactions in the MWCNTs bundles and leads to their **debundling** and dispersion. The increasing amount of MWCNT concentration resulted in an increasing value of the absorbance as shown in Figure 3, which gradually decreased from UV to near-IR. This decrease is also partly the result of scattering, especially in the lower wavelength range.

<Figure 3 near here>

Thermogravimetric analyses permitted to quantify the amount of MWNTs included in the PVBC_Et₃N matrix. A typical result of a thermogravimetric scan (Figure S1, suppl. info) showed polymer degradation at about 210 °C, with the loss of the ionic moieties, and at 425 °C, whereas the burning of the residual carbon nanotubes is activated at 600 °C when the purge gas is switched from nitrogen to air.

In Figure 4a, the weight percentage of MWNTs in the PVBC_Et₃N nanocomposite is reported as a function of the MWNT concentration. Measurements performed in triplicate showed only a 2% relative standard deviation. A 13 wt.% dispersion of MWNTs in the PVBC_Et₃N matrix was achieved for the MWCNT/PVBC_Et₃N 1:20 mixture. This amount suggests the excellent surfactant properties of the styrene-based ionomer, since equivalent MWCNT contents were previously obtained only with equiponderal mixtures of CNT and poly(styrene-*b*-(ethylene-co-butylene)-*b*-styrene) after 10 min of sonication.[12] This amount increased monotonically according to the UV-vis results shown in Figure 3, up to about 47.5 wt.% for the MWCNT/PVBC_Et₃N 1:1 experiment.

<Figure 4 near here>

It is worth noting that plotting the absorbance at the given wavelength of 400 nm against the w/w percentage concentration of MWCNTs (data from TGA, Figure 4a) demonstrates a linear correlation ($R^2 = 0.96$), especially in the low concentration regime (Figure 4b). A deviation from linearity at higher MWCNT concentration could be attributed to the stronger contribution of scattering phenomena. The slope of the fitting line, i.e. the apparent absorption coefficient, was calculated to be $0.018 \pm 0.002 \text{ mL}^{-1}$.

In order to evaluate if the dispersion process allowed the exfoliation of MWNTs, the MWCNT/PVBC_Et₃N mixtures were analyzed by atomic force microscopy (AFM). Figure 5 shows a representative AFM image of the MWCNT/PVBC_Et₃N 1:4 sample (19.3 wt.% of MWCNT) deposited on mica. The image clearly indicates that most of CNTs are exfoliated into small bundles less than 15 nm in diameter or even individual nanotubes. This result suggests the main role of the ionomer in promoting favorable interactions with MWCNTs, thus favoring their

debundling.

<Figure 5 near here>

Raman spectroscopy is a versatile technique to study carbon nanotube composition and possible degradation during processing.[25, 26] The most prominent features in a Raman spectrum of MWCNTs are the G and D bands (Figure 6). The G-band appeared near 1600 cm^{-1} and corresponds to planar vibration of carbon atoms of most graphite like materials. G-band is thus an intrinsic feature of CNTs, closely related to vibrations in all sp_2 carbon materials. The disorder-induced D-band appeared near 1310 cm^{-1} and was attributed to the scattering from defects, which break the basic symmetry of the graphene sheet. MWCNTs typically show the highest I_D/I_G ratio, since large amounts of structural defects are present due to its multiple graphite layers. In our case, a I_D/I_G ratio of 1.9 was calculated for the MWCNT/PVBC_Et₃N prepared both from 1:1 and 1:4 by weight mixtures in DMF, that was totally in agreement with the value of 2 measured for pristine MWCNTs.[27] This result indicates that the experimental set-up utilized for the preparation of MWCNT/PVBC_Et₃N nanocomposites did not affect the graphitic order on the MWCNTs surface, and further confirm that the limitation of the sonication time to 5 min preserves CNT structure.[12] Indeed, the so-called G' band ($\sim 2610\text{ cm}^{-1}$), associated with second-order sp_2 carbon feature and reflecting the metallic character in MWCNTs,[28] is well detectable in the spectrum.

<Figure 6 near here>

The electrical resistance of the composite was found to decrease according to the amount of MWNTs dispersed in the PVBC_Et₃N matrix (Figure 7).

<Figure 7 near here>

A strong variation of resistance, i.e. from $94.5\text{ k}\Omega$ to $2.6\text{ k}\Omega$, occurred for a relative small variation of MWCNT concentration, i.e. from 13.2 wt.% to 17.6 wt.%. After that, the resistance of the nanocomposite changed less markedly but still steadily, suggesting that the additional amount of dispersed nanotubes was still able to create new effective percolation pathways within the polymer matrix.

3.3 Resistance sensitivity to temperature

CNTs with either semi-conducting or metallic character show a resistivity that depends on temperature, which makes CNT nanocomposites potentially useful for the fabrication of temperature sensors.

<Figure 8 near here>

Figure 9 shows the calibration curves of sensors fabricated with MWCNT/PVBC_Et₃N dispersions containing different amounts of MWCNTs. A linear correlation of the resistance variation can be observed for all the prepared MWCNT/PVBC_Et₃N nanocomposites. More specifically, the sensors fabricated with the lowest MWCNT concentrations had the highest sensitivity corresponding to a negative temperature coefficient of about -0.004 K^{-1} , an absolute value that is comparable to the highest values found in metals ($0.0037\text{-}0.006\text{ K}^{-1}$; for example the value of 0.00385 K^{-1} corresponds to a Pt100 sensor).

The different MWCNT concentration led to differences in sensor performance, and the sensor prepared from MWCNT/PVBC_Et₃N dispersions containing the highest MWCNT concentration displayed a sensitivity about 1.5-2 times lower. This result is attributed to the fact that materials fabricated with MWCNT content close to the percolation threshold are characterized by largest resistance sensitivity to temperature.[29]

<Figure 9 near here>

An important feature of the prepared sensors is reported in figure 9, which illustrates the response of the MWCNT/PVBC_Et₃N 1:20 sensor to a sequence of heating and cooling cycles from 20 °C to 40 °C. It appears that the resistance of the sensor well recovers to the original value after the return to the room temperature, thus indicating the good reproducibility of the sensor response.

4. Conclusions

Well exfoliated MWCNT/polymer nanocomposites can be realized by using a new styrene-based ionomer, a poly(vinylbenzyl chloride) in which 78 % Cl atoms of the benzyl groups were replaced by Et₃N. The weight percentage of CNTs in MWCNT/PVBC_Et₃N nanocomposites can be easily modulated by varying the MWCNT concentration of DMF mixtures, as demonstrated by UV-vis experiments and TGA investigations. AFM microscopy and Raman spectroscopy evidenced the realization of well exfoliated and intimate polymer mixtures containing undamaged MWCNTs. The great dispersability of MWCNTs in PVBC_Et₃N was also reflected on the electrical resistance of nanocomposites, which showed a strong increase of conductivity for a relatively small variation of MWCNT concentration from 13.2 wt.% to 17.6 wt.%, thus suggesting the formation of highly percolative MWCNT/polymer networks.

The MWCNT/PVBC_Et₃N system displayed, for MWCNT contents close to the percolation threshold, a resistance sensitivity to temperature of -0.004 K^{-1} , an absolute value that is comparable to the highest values found in metals. It is worth to notice that the MWCNT/PVBC_Et₃N nanocomposite showed a very good reproducibility of the sensor response towards alternating heating and cooling cycles, thanks to the phase stabilization of the composite provided by the high T_g ionomer.

In conclusion, the results reported here indicated that such nanocomposite can be exploited for the realization of low-cost, small-sized and highly reproducible temperature sensors to be used in the range 20-40 °C. Future work will involve the optimization of the dispersion procedure of MWCNTs to best match the percolation threshold and thereby improve sensitivity. The possible influence of humidity on the sensor performances will be also investigated and a protecting polyimide tapes will be eventually utilized during assembly and throughout the life of the sensor.

Acknowledgements

The financial support of European Commission (FP7 Project 317894-SWAN-iCARE) is gratefully acknowledged. Dr. Michele Alderighi is acknowledged for his help in AFM measurements.

References

- [1] S. Iijima, *Nature*, 354 (1991) 56-58.
- [2] P.M. Ajayan, O. Stephan, C. Colliex, D. Trauth, *Science*, 265 (1994) 1212-1214.
- [3] J.M. Schnorr, T.M. Swager, *Chemistry of Materials*, 23 (2011) 646-657.
- [4] W.A. de Heer, *MRS Bulletin*, 29 (2004) 281-285.
- [5] M. Moniruzzaman, K.I. Winey, *Macromolecules*, 39 (2006) 5194-5205.
- [6] N.G. Sahoo, S. Rana, J.W. Cho, L. Li, S.H. Chan, *Progress in Polymer Science*, 35 (2010) 837-867.
- [7] F. Ciardelli, S. Coiai, E. Passaglia, A. Pucci, G. Ruggeri, *Polym. Int.*, 57 (2008) 805-836.
- [8] M.T. Byrne, Y.K. Gun'ko, *Advanced Materials*, 22 (2010) 1672-1688.
- [9] R.H. Baughman, A.A. Zakhidov, W.A. de Heer, *Science*, 297 (2002) 787-792.
- [10] K.L. Lu, R.M. Iago, Y.K. Chen, M.L.H. Green, P.J.F. Harris, S.C. Tsang, *Carbon*, 34 (1996) 814-816.
- [11] G. Matzeu, A. Pucci, S. Savi, M. Romanelli, F. Di Francesco, *Sensors and Actuators, A: Physical*, 178 (2012) 94-99.
- [12] N. Calisi, A. Giuliani, M. Alderighi, J.M. Schnorr, T.M. Swager, F. Di Francesco, A. Pucci, *European Polymer Journal*, 49 (2013) 1471-1478.
- [13] L. Vaisman, H.D. Wagner, G. Marom, *Advances in Colloid and Interface Science*, 128-130 (2006) 37-46.
- [14] R. Rastogi, R. Kaushal, S.K. Tripathi, A.L. Sharma, I. Kaur, L.M. Bharadwaj, *Journal of Colloid and Interface Science*, 328 (2008) 421-428.
- [15] V.C. Moore, M.S. Strano, E.H. Haroz, R.H. Hauge, R.E. Smalley, J. Schmidt, Y. Talmon, *Nano Letters*, 3 (2003) 1379-1382.
- [16] D.M. Delozier, D.M. Tigelaar, K.A. Watson, J.G. Smith Jr, D.J. Klein, P.T. Lillehei, J.W. Connell, *Polymer*, 46 (2005) 2506-2521.
- [17] J. Wang, M. Musameh, Y. Lin, *Journal of the American Chemical Society*, 125 (2003) 2408-2409.
- [18] M. Faraj, E. Elia, M. Boccia, A. Filpi, A. Pucci, F. Ciardelli, *Journal of Polymer Science, Part A: Polymer Chemistry*, 49 (2011) 3437-3447.
- [19] M. Faraj, M. Boccia, H. Miller, F. Martini, S. Borsacchi, M. Geppi, A. Pucci, *International Journal of Hydrogen Energy*, 37 (2012) 14992-15002.
- [20] A. Filpi, M. Boccia, A. Pucci, F. Ciardelli, *e-Polymers*, (2013) 001.
- [21] M. Piana, M. Boccia, A. Filpi, E. Flammia, H.A. Miller, M. Orsini, F. Salusti, S. Santuccioli, F. Ciardelli, A. Pucci, *Journal of Power Sources*, 195 (2010) 5875-5881.
- [22] G.A. Rance, D.H. Marsh, R.J. Nicholas, A.N. Khlobystov, *Chem. Phys. Lett.*, 493 (2010) 19-23.
- [23] F. Wang, G. Dukovic, L.E. Brus, T.F. Heinz, *Science*, 308 (2005) 838-841.
- [24] S. Attal, R. Thiruvengadathan, O. Regev, *Analytical Chemistry*, 78 (2006) 8098-8104.
- [25] R. Gao, S.M. Ramirez, D.L. Inglefield, R.J. Bodnar, T.E. Long, *Carbon*, 54 (2013) 133-142.
- [26] M.A. Pimenta, G. Dresselhaus, M.S. Dresselhaus, L.G. Cancado, A. Jorio, R. Saito, *Physical Chemistry Chemical Physics*, 9 (2007) 1276-1290.

- [27] Z. Morávková, M. Trchová, E. Tomsík, J. Cechvala, J. Stejskal, *Polymer Degradation and Stability*, 97 (2012) 1405-1414.
- [28] M.S. Dresselhaus, A. Jorio, M. Hofmann, G. Dresselhaus, R. Saito, *Nano Letters*, 10 (2010) 751-758.
- [29] S.H. Foulger, *Journal of Applied Polymer Science*, 72 (1999) 1573-1582.

Figure captions

Figure 1. FT-IR spectra of PVBC and PVBC_Et₃N

Figure 2. ¹H NMR spectrum of PVBC (a) and magnified region from 4.20 to 4.70 of ¹H NMR spectra of PVBC and PVBC_Et₃N (b). The dotted curves were obtained after peak deconvolution and fitting by least-squares method ($R^2 = 0.998$).

Figure 3. Representative absorption spectra of MWCNT/PVBC_Et₃N DMF dispersions as a function of MWNT loading and PVBC_Et₃N DMF solution (0.4 wt.%)

Figure 4. (a) Amount of MWNTs (wt.%) dispersed within PVBC_Et₃N; and (b) plot of absorbance value recorded at 400 nm as a function of MWCNTs concentration (wt.%)

Figure 5. AFM image of MWCNT/PVBC_Et₃N nanocomposite prepared from a 1:4 by weight mixture in DMF

Figure 6. Raman spectra of MWCNT/PVBC_Et₃N prepared from 1:1 (straight line, 47.5 wt.% of MWCNT) and 1:4 (dashed line, 19.3 wt.% of MWCNT) by weight mixtures in DMF ($\lambda_{\text{exc.}} = 785$ nm)

Figure 7. Logarithmic scale plot of the electrical resistance of MWCNT/PVBC_Et₃N as a function of MWCNT concentration

Figure 8. Percentage variation of resistance versus temperature for MWCNT/PVBC_Et₃N nanocomposites obtained from dispersions at different MWCNT concentration

Figure 9. for MWCNT/PVBC_Et₃N prepared from 1:20 (13.2 wt.% of MWCNT) by weight mixture

Schemes and figures

Figure 1

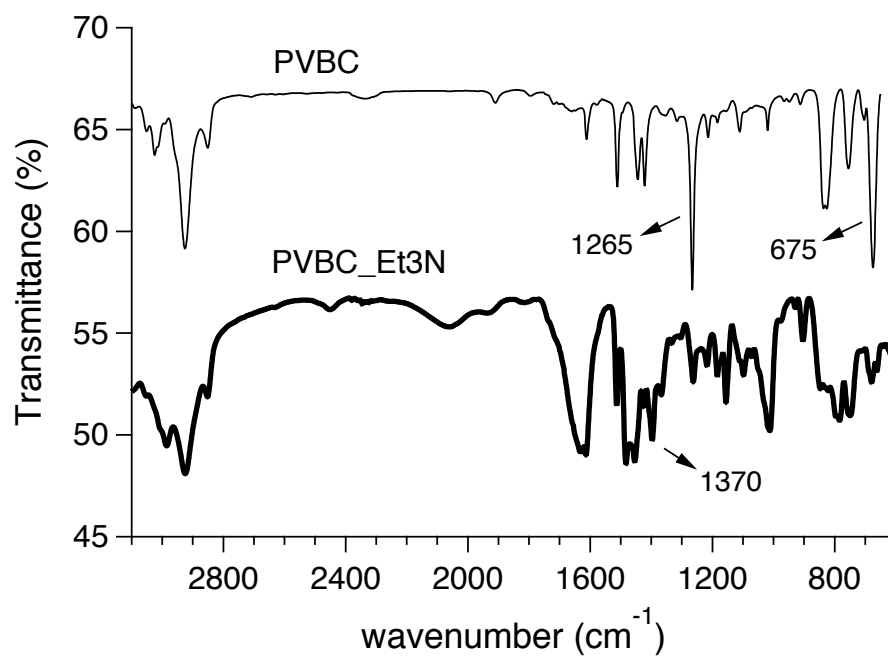
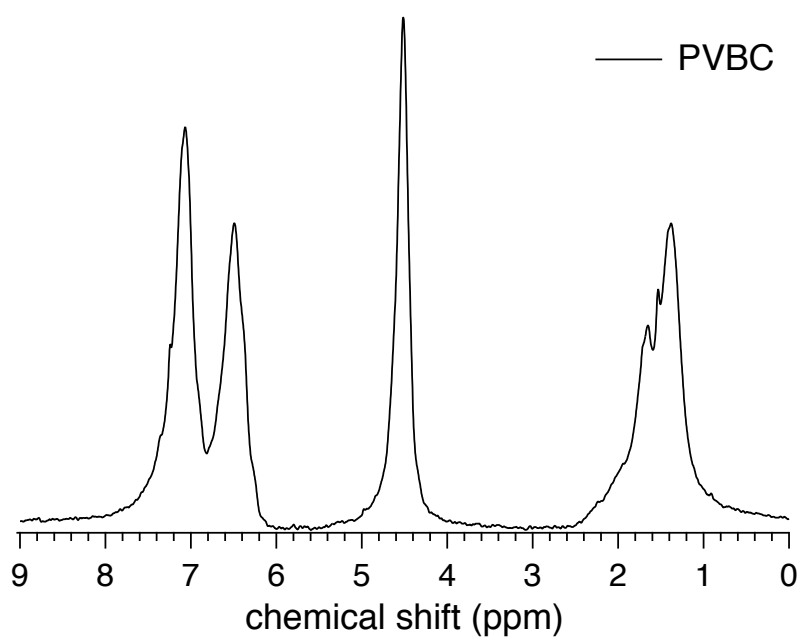
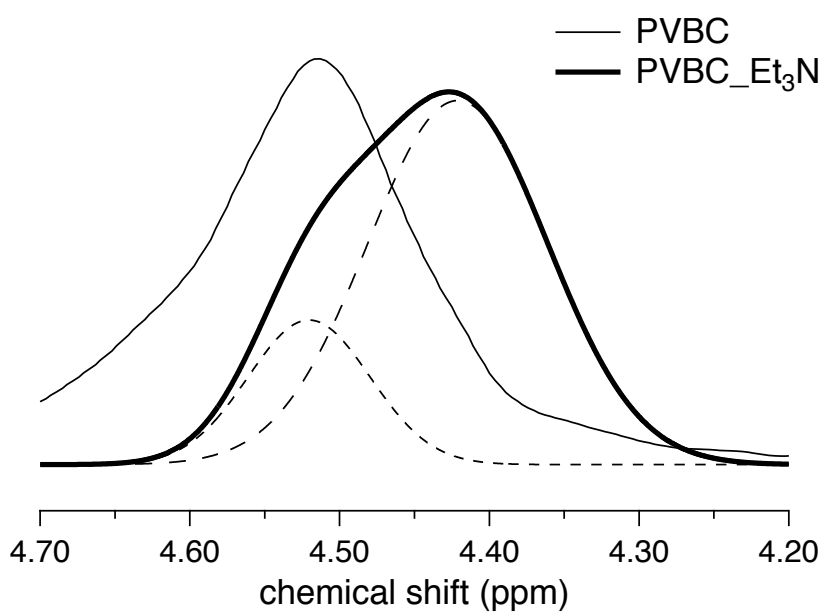


Figure 2



(a)



(b)

Figure 3

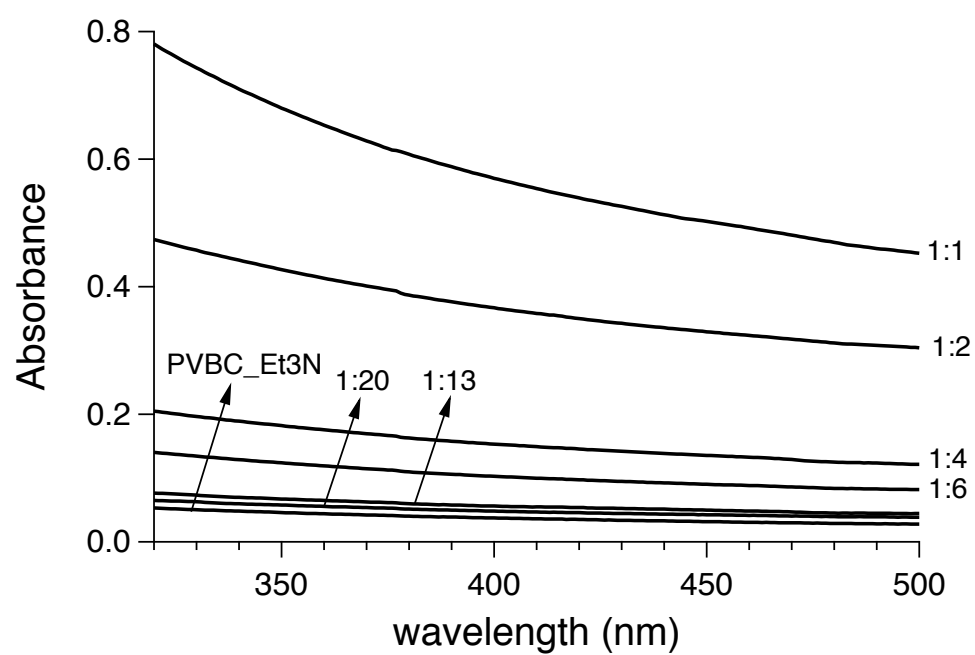


Figure 4

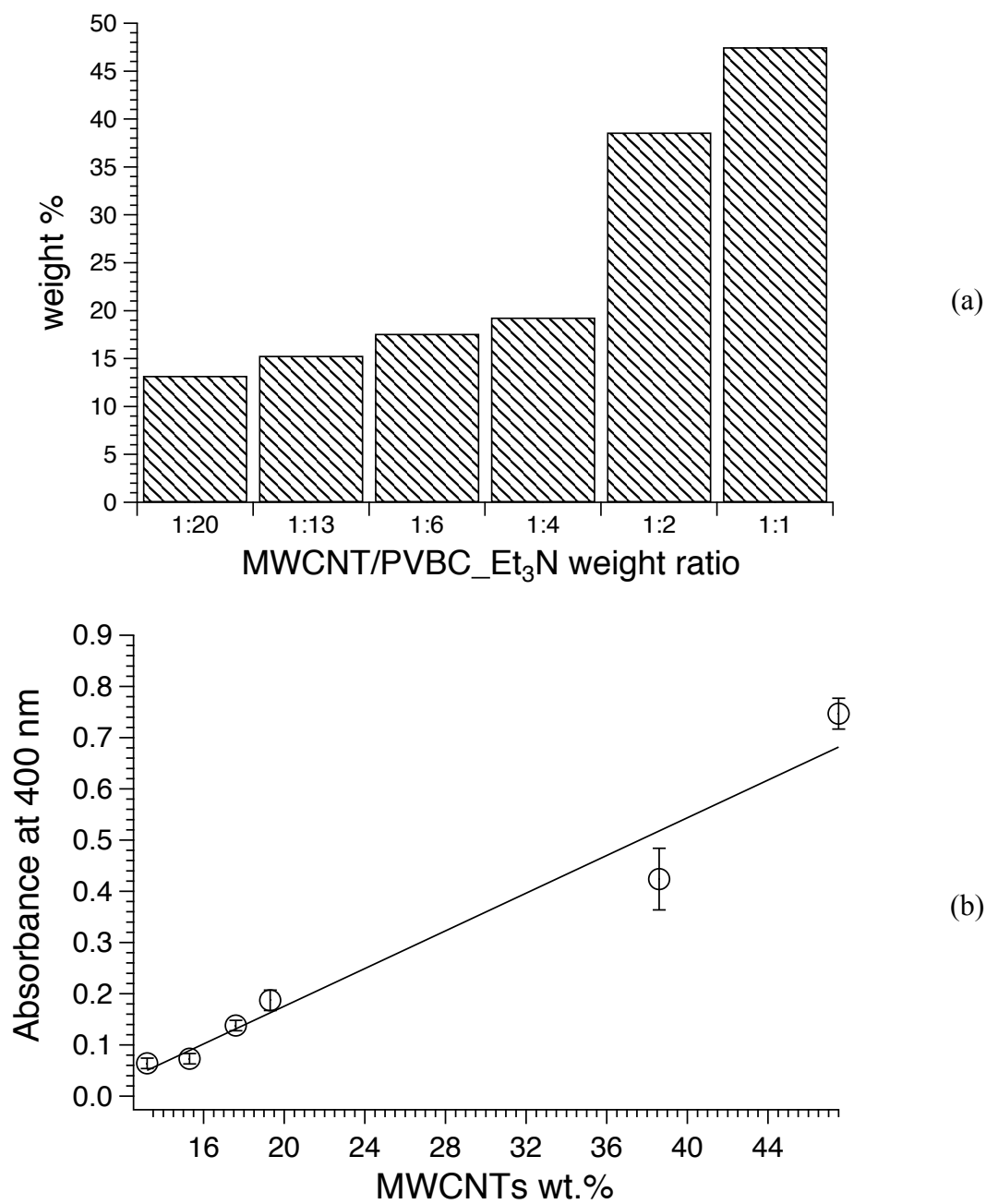


Figure 5

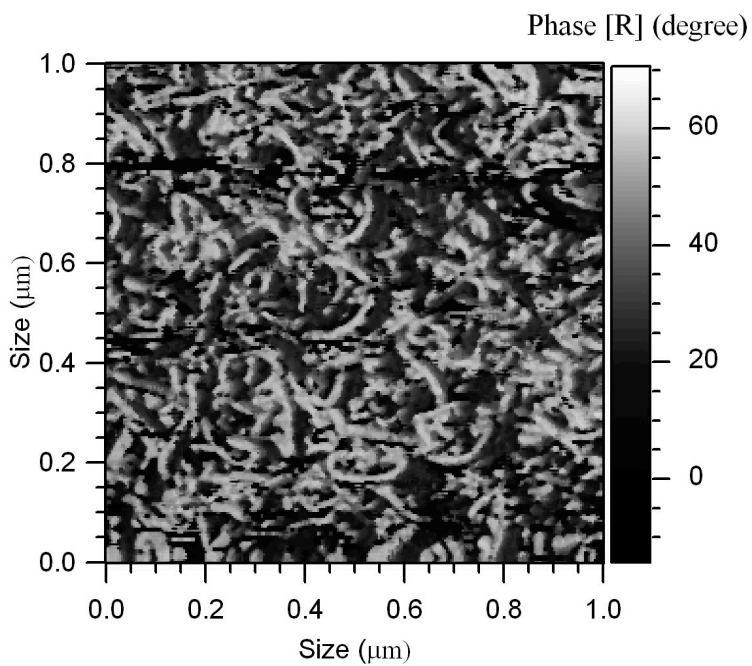


Figure 6

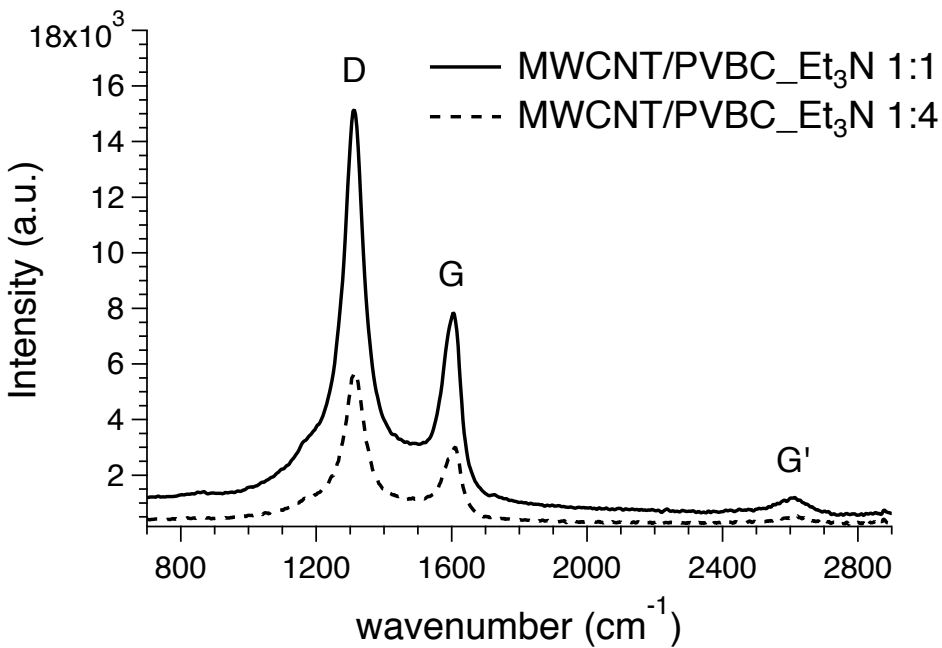


Figure 7

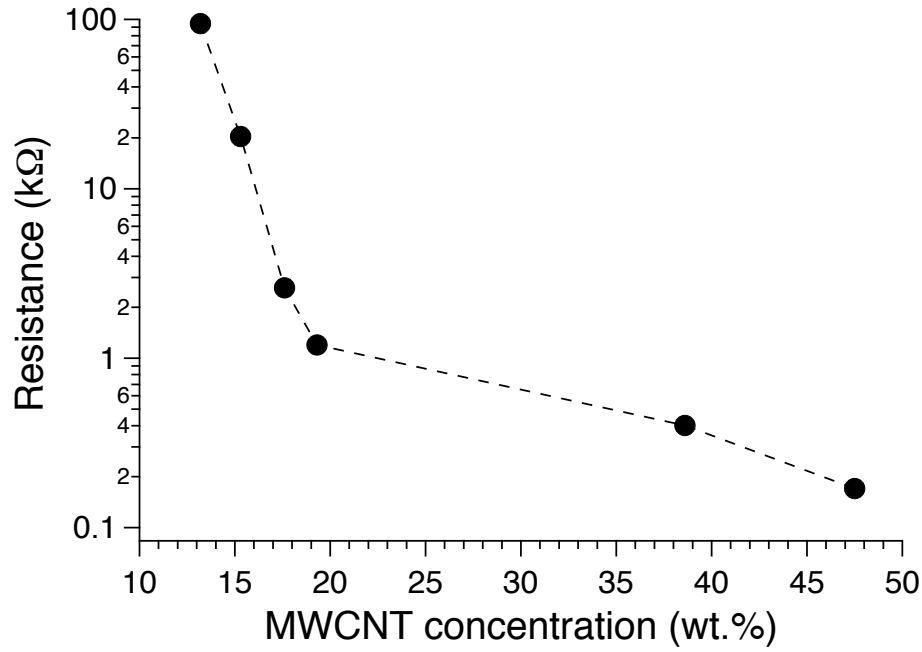


Figure 8

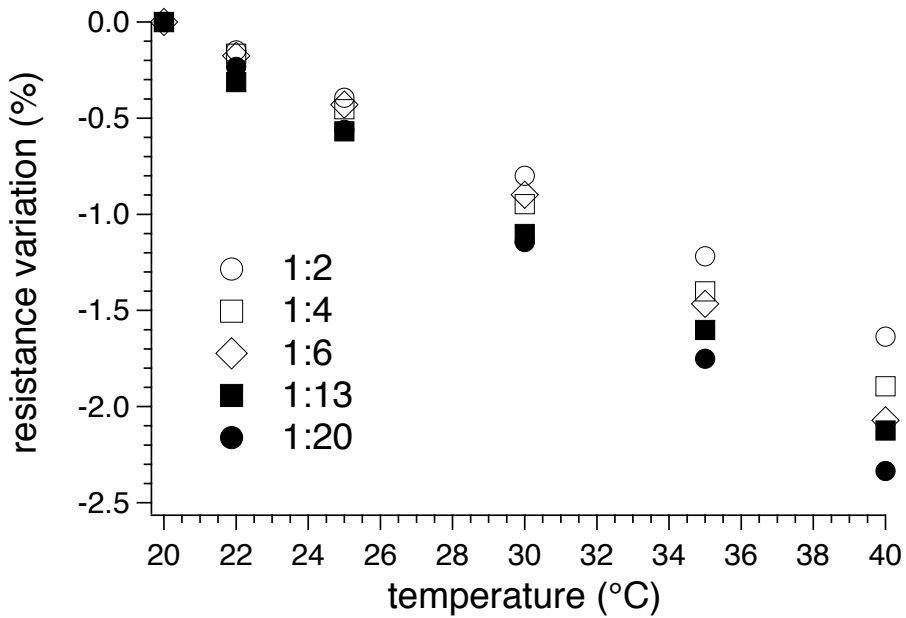
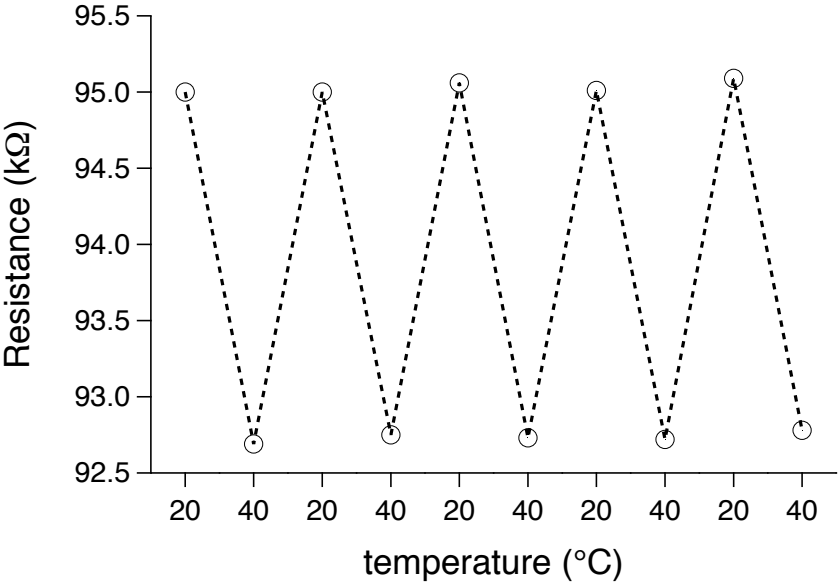


Figure 9



Supplementary information

Alessio Giuliani, Massimo Placidi, Fabio Di Francesco, Andrea Pucci

“A New Polystyrene-based Ionomer/MWCNT Nanocomposite for Wearable Skin Temperature Sensors”

Figure S1. Representative thermogravimetric scan of a MWCNT/PVBC_Et₃N nanocomposite with a nanotube weight percentage of about 40%.

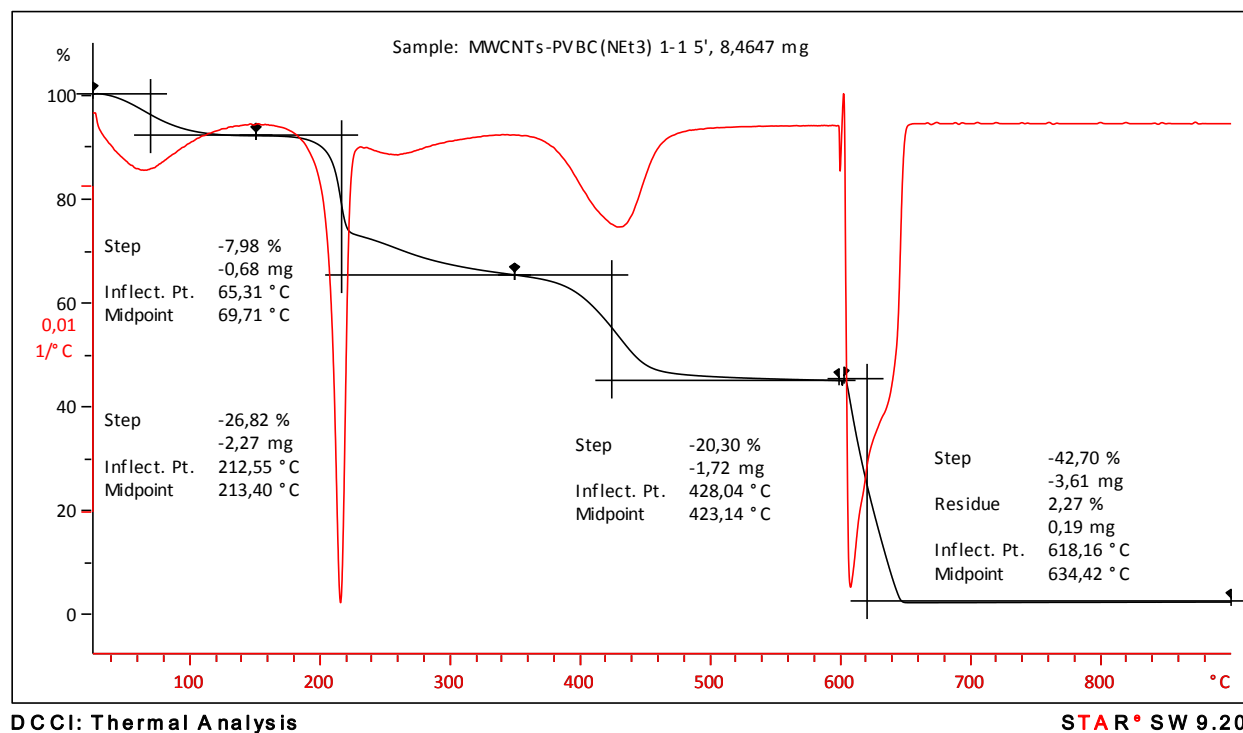


Figure S2. Schematic diagram of the sensor: (a) section and (b) top view

